

CFNet: Learning Correlation Functions for One-Stage Panoptic Segmentation

Yifeng Chen^{1*}, Wenqing Chu^{2*}, Fangfang Wang¹, Ying Tai²,
Ran Yi³, Zhenye Gan², Liang Yao², Chengjie Wang², Xi Li¹

¹Zhejiang University, ²Tencent Youtu Lab, ³Shanghai Jiao Tong University

Abstract

Recently, there is growing attention on one-stage panoptic segmentation methods which aim to segment instances and stuff jointly within a fully convolutional pipeline efficiently. However, most of the existing works directly feed the backbone features to various segmentation heads ignoring the demands for semantic and instance segmentation are different: The former needs semantic-level discriminative features, while the latter requires features to be distinguishable across instances. To alleviate this, we propose to first predict semantic-level and instance-level correlations among different locations that are utilized to enhance the backbone features, and then feed the improved discriminative features into the corresponding segmentation heads, respectively. Specifically, we organize the correlations between a given location and all locations as a continuous sequence and predict it as a whole. Considering that such a sequence can be extremely complicated, we adopt Discrete Fourier Transform (DFT), a tool that can approximate an arbitrary sequence parameterized by amplitudes and phases. For different tasks, we generate these parameters from the backbone features in a fully convolutional way which is optimized implicitly by corresponding tasks. As a result, these accurate and consistent correlations contribute to producing plausible discriminative features which meet the requirements of the complicated panoptic segmentation task. To verify the effectiveness of our methods, we conduct experiments on several challenging panoptic segmentation datasets and achieve state-of-the-art performance on MS COCO with 45.1% PQ and ADE20k with 32.6% PQ.

1. Introduction

Panoptic segmentation [20], a fundamental and challenging problem in scene parsing, is to carry out instance segmentation for foreground things and semantic segmentation for background stuff. In recent years, a large number of approaches [19, 35, 54, 12, 34] have been proposed for panoptic segmentation due to its wide potential appli-

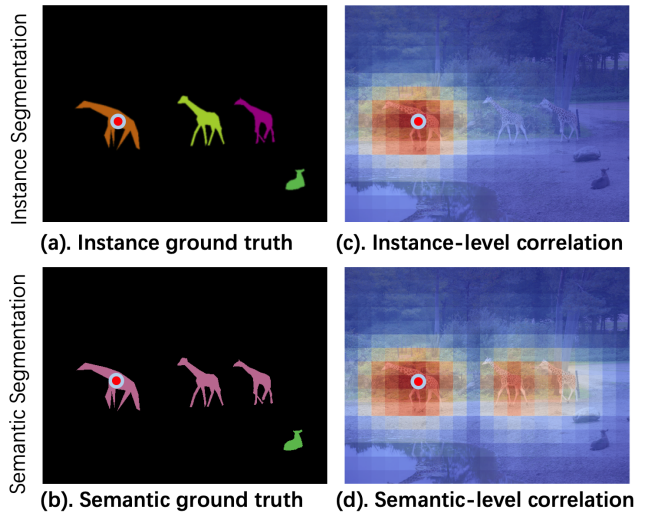


Figure 1: Visualizations of different correlations with respect to a given point (red point), where red color represents higher correlation. (a), (b) are ground truth for instance and semantic segmentation. (c), (d) are correlations modeled by the proposed function. Our mechanism is able to model correlations from scenes directly, showing a scene-related task-specific result in (c) and (d).

cations in autonomous driving, robotics, and image editing. Among these algorithms, the workflow of one-stage methods [10, 24, 16] also referred to box-free is simple and effective which attracts large attention.

Current one-stage methods usually leverage a Feature Pyramid Network [25] based backbone to extract feature maps and then attach different segmentation heads to them. However, we note that the demands for semantic and instance segmentation are different: The former needs discriminative features across different categories, while the latter requires features to be instance-level distinguishable. To alleviate this, the attention mechanism is introduced to help semantic segmentation [44, 2], which can enhance the semantic consistency within the same class. For the instance segmentation, coordinates [41, 2, 28] are typically concatenated with the backbone feature maps for capturing spatial cues which have been proven to be effective

*Equal Contribution.

for enhancing instance-level discrimination to some degree. From a unified view, the attention mechanism and CoordConv [28] both aim to introduce discriminative features, while the former is for semantic-level and the latter is instance-level. Unfortunately, these features are heuristic or fixed that are not flexible insufficient for various scenes, e.g., discrimination should be stricter for more crowded scenes in instance segmentation.

In this work, we propose to predict semantic-level and instance-level correlations and then utilize this information to guide the feature enhancement for efficient panoptic segmentation. Specifically, we treat these correlations as task-driven and scene-relevant so that we could learn them through implicit supervisions from tasks. As shown in Fig. 1, we organize the correlations between a given location and all locations as a sequence and learn it as a whole. In other words, we seek to learn a function with coordinates as input to approximate this sequence. It is more sensible than learning correlations individually since the latter ignores the fact that two adjacent locations tend to have continuous correlations. Meanwhile, we note that such a sequence can be extremely complicated, which requires a powerful function family to cover it. To meet these requirements, we adopt DFT (Discrete Fourier Transform [32]), a tool that can approximate an arbitrary sequence to the addition of several sinusoidal base functions parameterized by amplitudes and phases. Moreover, we introduce a convolutional module to predict the function parameters for capturing different kinds of correlations in various segmentation tasks. This module leverages the scene content as input and is optimized implicitly by corresponding tasks.

With the predicted correlations, we can improve the backbone features effectively. For semantic segmentation, we directly aggregate those pixel features within the same semantic to enhance the discrimination. For instance segmentation, we stack the pixel correlations with other locations as discriminative features and concatenate them with the backbone features to improve the discrimination. As a result, different segmentation heads could obtain plausible inputs and generate the segmentation results accurately.

The main contributions of our work are as follows:

- We introduce a new DFT based correlation function which is able to model task-specific, scene-related correlations among different locations flexibly.
- We point out that one-stage panoptic segmentation needs different kinds of feature discrimination and propose to learn the correlation function parameters in a convolutional manner which is inserted into the one-stage panoptic segmentation pipeline seamlessly.
- We conduct extensive experiments to analyze the proposed method which obtains SOTA panoptic segmentation performance with 45.1% PQ on MS COCO and 32.6% on ADE20k.

2. Related Work

Semantic segmentation. Semantic segmentation, a task of pixel-wise classification, has seen great progress since the emergence of fully convolutional network [30]. Various methods have been proposed to make use of beneficial context information. PSPNet [55] adopts pyramid modules to exploit multi-scale features. Atrous [4, 5, 6] and deformable convolutions [11] improve the sampling process of vanilla convolutions. The attention mechanism [37, 18] considers the pixel-to-pixel relationship as non-local and designs a global feature broadcast scheme based on semantic affinities. Meanwhile, several methods [57, 45, 56] introduce explicit correlation based constraints on the semantic predictions to capture image structure information.

Instance segmentation. Instance segmentation targets to assign a category and an instance ID to each object pixel. Two-stage methods, represented by Mask-RCNN [14], generate region proposals in the first stage and segment them in the second stage. One-stage methods seek ways to model masks densely. TensorMask [7] directly learns instance masks as flattened vectors, while SOLO [41] reduces its complexity by dividing the input into uniform grids. Contour-based methods [47, 49] parameterize masks by polynomials fitting and learn the internal parameters instead. Embedding-based methods [31, 53] extract masks by learning pixel and proposal embedding, while CondInst [36] and SOLOv2 [43] take a further step by introducing dynamic convolutions [50].

Panoptic segmentation. Panoptic segmentation [20] is a joint task of instance segmentation and semantic segmentation. Two-stage methods [19, 33] extend Mask-RCNN with a fully convolutional branch and apply a heuristic fusion algorithm [20] to fuse instances and stuff predictions. Lots of efforts have been paid to building connections among tasks to leverage reciprocal information [9, 23, 46]. To improve the fusion process, both learnable [21, 27, 52] and parameter-free [22, 48] modules are proposed to deal with overlapping. One-stage methods [3, 8], on the other hand, focus on finding efficient ways to segment instances and stuff jointly within a fully convolutional pipeline. Embedding-based methods [13, 17, 29] extract instance masks by comparing the affinity between mask embeddings and instance embeddings. Voting-based methods [10, 38, 39] obtain masks through hough voting [1] by learning object centers and pixel-wise offsets. [42] incorporates semantic features into instance segmentation and leverages instance embeddings for enhancing semantic segmentation. However, all these instance-level discrimination enhancement modules are static, which will hurt their generalizability to various scenes. Instead, we seek to model different correlations adaptively and continuously. We propose correlation functions to model such correlation as

scene-relevant and improve feature representations in various segmentation tasks.

3. Proposed Method

In this section, we describe the proposed efficient one-stage pipeline for panoptic segmentation in detail. We first show the overall framework and then introduce different components. To alleviate the conflicts between different segmentation needs, we elaborate on the adapted and continuous correlation functions which are utilized to guide the learning for task-specific discriminative features. After that, two applications of correlations, namely Semantic Correlation Module (SCM) and Instance Correlation Module (ICM), are designed respectively for semantic and instance segmentation.

3.1. Architecture

To pursue both speed and accuracy, we employ a single-stage pipeline for panoptic segmentation, which contains four parts, including a backbone feature extractor, an instance segmentation branch with ICM and a semantic segmentation branch with SCM, and a post-processing algorithm to obtain panoptic results. The overall architecture of our method is shown in Fig. 2.

Backbone feature extractor. Backbone feature extractor aims to extract shared features for subsequent tasks. We adopt ResNet [15]+FPN [25] as the backbone network, where the outputs from different blocks of a ResNet are fed into a feature pyramid network to obtain multi-scale features, namely P_2, P_3, P_4, P_5 . An extra P_6 is included for instance segmentation by down-sampling P_5 .

Instance segmentation branch. Instance segmentation branch enriches the features from $\{P_i | i = 2, \dots, 6\}$ by ICM and performs instance segmentation at each level. For different levels, the weights of ICM are shared. Our ICM is a compatible module that can easily be plugged into various one-stage instance segmentation methods. In our work, we transplant the instance branch from pioneering SOLOv2 [43] to perform instance segmentation.

Semantic segmentation branch. Semantic segmentation branch takes $\{P_i | i = 2 \dots 5\}$, augments them by SCM and performs semantic segmentation. For different levels, the weights of SCM are shared. Following UPSNet [48], we design a subnet consisting of 4 stacked 3×3 convolutions. This subnet is applied to each pyramid level. After that, the output features are upsampled and concatenated to predict semantic segmentation.

Training and inference. To train our model, there are three loss terms in total:

$$L = \underbrace{L_{\text{mask}} + L_{\text{cate}}}_{\text{instance segmentation loss}} + \underbrace{\lambda L_{\text{sem}}}_{\text{semantic segmentation loss}}, \quad (1)$$

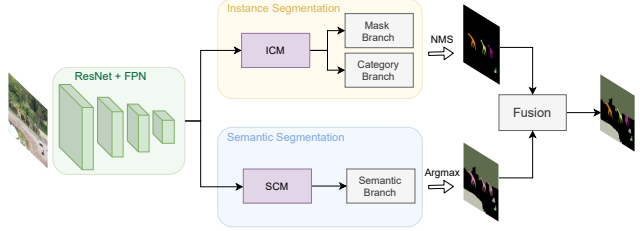


Figure 2: Architecture of the proposed one-stage panoptic segmentation pipeline, which contains four parts: a backbone feature extractor, an instance segmentation branch with ICM, a semantic segmentation branch with SCM, and a post-processing step for generating segmentation results.

where λ is used to control the balance between tasks. L_{mask} and L_{cate} are dice and focal loss following [41, 43]. L_{sem} is cross entropy loss for semantic segmentation. Parameters of SCM are optimized by semantic segmentation loss, while those of ICM are guided by instance segmentation loss. During inference, points with category scores higher than a certain threshold are first picked. Afterwards, a Matrix-NMS [41] is applied to remove duplicate predictions. Finally, a heuristic algorithm [20] fuses instance and semantic segmentation results to obtain the final panoptic output.

3.2. Correlation Functions

Here we introduce how to obtain the correlations applied in SCM and ICM. Both instance and semantic correlations are pixel-wise and exist between a given location i and all other locations. Previous practice of utilizing appearance similarity or coordinates to compute correlations brings two drawbacks: 1). It does not take the image as a whole and ignore the continuity of the correlations of a specific location with other locations. 2). It overlooks the image content that can be too rigid for various scenes. Hence, we propose the correlation function mechanism to directly model the underlying correlations as scene-relevant and tunes them to fit task needs through implicit supervisions.

Sequence decomposition. Given a 1-dimensional input of length L , we denote the correlation between location i and j as $cor(i, j)$. Our target is to learn $cor(i, j)$ for arbitrary i and j with merely implicit task supervisions. This makes directly learning $cor(i, j)$ infeasible since optimizing each $cor(i, j)$ independently without explicit losses is extremely difficult. To alleviate this, we hope to organize relevant correlations together and learn them as a whole to capture their internal distribution as shown in Fig. 3. Specifically, we view the correlations between a given location i and all other locations as a whole, and denote it by C_i :

$$C_i = [cor(i, 0), \dots, cor(i, L - 1)]. \quad (2)$$

C_i has the useful “continuity” property since the correlations between i and any two adjacent locations ought

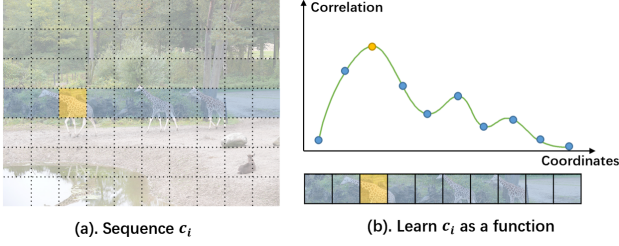


Figure 3: Illustration of correlation function. (a) demonstrates the concept of sequence c_i in a real scenario, while (b) gives out a case of a possible sequence c_i under this scenario and shows that a function of coordinates can be used to approximate it.

to be close as nearby locations have similar contents. In other words, C_i can be approximated as the output of discrete sampling on a hidden continuous function of locations. By doing so, the dense $L \times L$ correlation learning issue is decomposed to the learning of L sequences $\{C_0, C_1, \dots, C_{L-1}\}$, where each C_i can be further learned as a whole by a approximation function.

Sequence learning. We denote the approximation function of C_i as $\mathcal{G}(\theta_i, j)$, where θ_i are parameters and j are coordinates. The learning of variable-length C_i is now converted to the learning of a fixed number of parameters θ_i . Due to the fact that C_i can be of arbitrary forms related to the specific scene content and task requirements, \mathcal{G} must be powerful enough to cover any possible cases. Hence, we adopt DFT (Discrete Fourier Transform), which is known for its capability to fit any discrete sequences. To meet its prerequisite, we first extend C_i to a form a periodic signal T_i of frequency $\omega = 2\pi/L$ by having:

$$T_i[j] = C_i[j \bmod L]. \quad (3)$$

This extension leads to an issue that the beneficial ‘‘continuity’’ breaks between $T_i[L-1]$ and $T_i[0]$, where these two locations, i.e., the start and end of the signal, tend to have different correlations with location i . To avoid this, we append C_i with its mirrored signal to form C'_i before extending it to periodic signal $T'_i(t)$:

$$C'_i[j] = \begin{cases} C_i[j] & 0 \leq j < L \\ C_i[2L-j-1] & L \leq j < 2L. \end{cases} \quad (4)$$

After obtaining the periodic discrete signal T'_i of frequency $\omega' = \omega/2$, DFT approximates it as an addition of N base sinudual functions parameterized by amplitudes A_n^i and phrases ψ_n^i as follows:

$$T'_i(j) \approx A_0^i + \sum_{n=1}^N A_n^i \sin(n\omega'j + \psi_n^i) \stackrel{\text{def}}{=} \mathcal{G}(\theta_i, j), \quad (5)$$

where $\theta_i = \{A_0^i\} \cup \{A_n^i, \psi_n^i | n = 1, \dots, N\}$. To utilize the knowledge that the concrete form of this function (i.e., sequence) varies with scenes, we choose to predict θ_i from signal contents. For L sequences, there are $L \times (2N + 1)$ parameters in total, where N is the level of expansion in Eq. 5. This is implemented through conventional convolutions, where feature of each location i is responsible to predict θ_i to generate the correlation sequence C_i . Afterwards, C_i will be used along with signal content to fulfill tasks so that θ_i can be optimized under implicit supervisions.

2-dimensional extensions. Extending the 1-dimensional signal of L to 2-dimensional (2d) inputs of $H \times W$ is non-trivial since the assumption of continuity breaks when row or column changes. Nevertheless, for locations belonging to the same row or column, such an assumption still exists. Hence, we choose to approximate the function of 2-dimensional locations as the product of two independent axial 1-dimensional functions:

$$\begin{aligned} cor_{2d}(u, v) &= cor_{hor}(u, v) \cdot cor_{ver}(u, v) \\ &= \mathcal{G}(v_x, \theta_u^{hor}) \cdot \mathcal{G}(v_y, \theta_u^{ver}), \end{aligned} \quad (6)$$

where u, v are two 2d locations, v_x and v_y are the coordinates of location v along horizontal and vertical axis. And $\theta_u = [\theta_u^{hor}, \theta_u^{ver}]$ are the parameters of two axial 1-dimensional functions. The learning of $H \times W \times H \times W$ correlations are now converted to $H \times W \times 2$ sets of parameters, where each contains $2N + 1$ variables. Similarly, the total $H \times W \times 2(N + 1)$ is predicted by applying convolutions upon input features and receives supervision from implicit tasks losses.

Discussions with the decoupled SOLO [41]. We decompose dense correlation predictions to two orthogonal function learning, while decoupled SOLO predicts two dense 1d tensors. However, the underlying motivations are distinct. Decoupled SOLO decomposes dense prediction for efficiency, while we are to make use of ‘‘spatial locality’’, i.e, we want adjacent locations of similar positional correlation. If we learn a single function to predict the 2d correlation, the end of row i will get similar correlations as the start of row $i + 1$ since they are considered ‘‘adjacent’’ in the flatten 1d view. (No matter how you flats, the ‘‘false adjacent’’ issue will still exist). One would not want that since the two ends of one image tend to be irrelevant.

3.3. Application of Correlations

With the proposed correlation functions, we are able to model correlations directly from scene inputs. In this section, we introduce two modules, namely Semantic Correlation Module (SCM) and Instance Correlation Module (ICM), to make use of such correlation respectively in semantic segmentation and instance segmentation, two sub-tasks of panoptic segmentation.

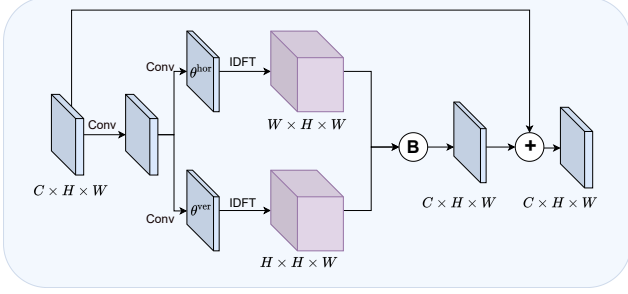


Figure 4: Structure of semantic correlation module. B represents the broadcast process in Eq. 9, and \oplus indicates element-wise addition.

Semantic correlation module. To learn semantic-level discriminative features, the design of semantic correlation module (SCM) follows the spirit of how attention mechanism [39, 44] are applied in semantic segmentation [37]. Recall that in the original attention mechanism, one defines the correlation between one location u and location v as:

$$w_{u,v} = f_u^T Q K^T f_v = f_u^T M f_v, \quad (7)$$

where $M = Q K^T$, Q and K are projection matrices, f_u and f_v are visual features at location u and v . Naturally, our SCM replaces $w_{u,v}$ with $cor_{2d}(u, v)$, which can model scene-related, task-specific semantic-level correlation directly from scenes. It not only saves the trouble for time-consuming attention operations, but also enables the learning of complicated patterns. As shown in Fig. 4, our SCM applies a single 3×3 convolution on the input features and predicts $\theta_u = [\theta_u^{hor}, \theta_u^{ver}]$ densely by two 1×1 convolutions. Afterwards, $cor_{2d}(u, v)$ is calculated following Eq. 5 and Eq. 6. As for feature propagation, we provide two modes, namely global aggregation and axial aggregation. The former one aggregates information from all locations as:

$$f_u^S = \sum_v \text{softmax}_v(cor_{2d}(u, v)) f_v \quad (8)$$

The latter one gathers information from axial locations as:

$$f_u^S = \sum_{v \in \{p | p_x = u_x\}} \text{softmax}_v(cor_{hor}(u, v)) f_v + \sum_{v \in \{p | p_y = u_y\}} \text{softmax}_v(cor_{ver}(u, v)) f_v. \quad (9)$$

The enhanced feature f_u^S is used to perform semantic segmentation while θ_u can be optimized through the supervision from semantic segmentation. Taking efficiency into consideration, Axial aggregation mode is chosen for SCM.

Instance correlation module. Directly adopting the above semantic correlation mechanism for instance segmentation is not reasonable, because the aggregated features for different instances belonging to the same category

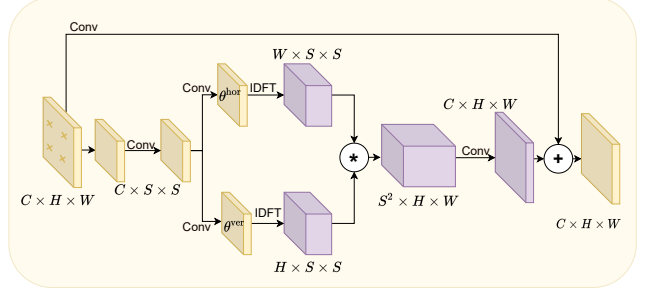


Figure 5: Structure of instance correlation module. S^2 reference points are uniformly sampled.

could still be very similar. Here, we hope to achieve instance discrimination which means the modification for different instances should be different. We find that if two locations are belonging to the same instance, then their correlations with other locations would be similar. Therefore, the correlations themselves could be viewed as discriminative features to make different instances distinguishable. This can help instance segmentation to tell instances apart. To be more specific, we concatenate the correlations of a given location and combine them with the visual features. Our ICM combines concatenated correlations with semantic features using the same addition operations. We sample C fixed locations as references, denoted as P , in the input and calculate the correlation of each location u with respect to these C reference locations as c_u :

$$c_u = [cor_{2d}(u, P_1), \dots, cor_{2d}(u, P_C)]^T. \quad (10)$$

Afterwards, it is directly added to visual features as:

$$f_u^I = W_f^T f_u + c_u \quad (11)$$

In practice, instead of sampling all points, we choose $S \times S$ points instead for efficiency. To match S^2 with C , a further 1×1 convolution is applied. The whole process of instance correlation module is illustrated in Fig. 5. The enhanced feature F^I is later used to perform instance segmentation.

4. Experiments

In this section, we evaluate our methods on challenging benchmarks COCO [26] and ADE20k [58]. In addition, we perform extensive ablation studies to verify the effectiveness of different components.

Datasets. MS COCO is a large-scale panoptic segmentation dataset with 118k training images, 5k validation images, and 20k test images. Annotations of 80 thing categories and 53 stuff categories for both instance segmentation and semantic segmentation are provided. We train our model on the *train* set without extra data and report results

method	Backbone	PQ	SQ	RQ	PQ Th	SQ Th	RQ Th	PQ St	SQ St	RQ St	FPS
<i>two-stage</i>											
Panoptic-FPN [19]	Res50-FPN	39.0	-	-	45.9	-	-	28.7	-	-	-
UPSNet [48]	Res50-FPN	42.5	78.0	52.5	48.6	79.4	59.6	33.4	75.9	41.7	9.1
BANet [9]	Res50-FPN	43.0	79.0	52.8	50.5	81.1	61.5	31.8	75.9	39.4	-
BRGNet [46]	Res50-FPN	43.2	-	-	49.8	-	-	33.4	-	-	-
Unifying [22]	Res50-FPN	43.4	79.6	53.0	48.6	-	-	35.5	-	-	-
CIAE [13]	Res50-FPN	40.2	-	-	45.3	-	-	32.3	-	-	12.5
SOGNet [52]	Res50-FPN	43.7	78.7	53.5	50.6	-	-	33.2	-	-	-
<i>one-stage</i>											
DeeperLab [51]	Xception-71	33.8	-	-	-	-	-	-	-	-	10.6
RealTimePan [17]	Res50-FPN	37.1	-	-	41.0	-	-	31.3	-	-	15.9
PCV [38]	Res50-FPN	37.5	77.7	47.2	40.0	-	-	33.7	-	-	5.7
Panoptic-Deeplab [10]	Xception-71	39.7	-	-	43.9	-	-	33.2	-	-	7.6
SOLOv2 [43]	Res50-FPN	42.1	-	-	49.6	-	-	30.7	-	-	-
LPSNet [16]	Res50-FPN	42.4	79.2	52.7	48.0	35.8	-	-	-	-	6.8
Panoptic-FCN [24]	Res50-FPN	43.6	80.6	52.6	49.3	82.6	58.9	35.0	77.6	42.9	12.5
Panoptic FCN* [24]	Res50-FPN	44.3	80.7	53.0	50.0	83.4	59.3	35.6	76.7	43.5	9.2
Ours	Res50-FPN	44.5	79.8	54.0	52.1	82.8	62.1	33.1	75.2	41.7	13.3
Ours*	Res50-FPN	45.1	81.0	54.4	51.8	82.8	61.7	35.1	78.2	43.5	10.5

Table 1: Results on COCO *val* set.

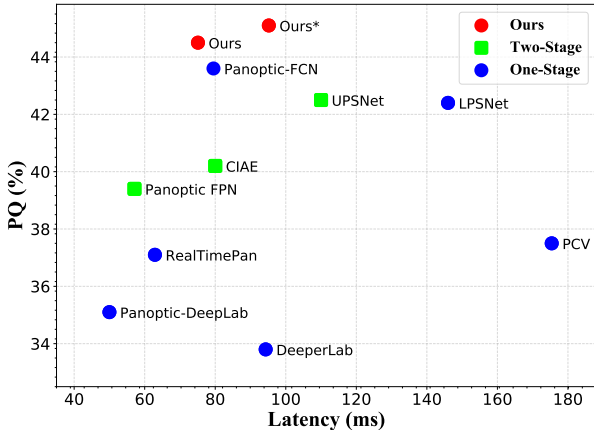


Figure 6: PQ and latency on COCO *val* set. Our method achieves state-of-the-art performance while keeping a competitive inference speed.

on both *val* and *test-dev* sets. ADE20K is a densely annotated dataset for panoptic segmentation containing 20k images for training, 2k images for validation and 3k images for test. It contains 150 classes in total, including 100 things and 50 stuff classes. We train our model on its *train* set without extra data and report results on its *val* set. We utilize PQ [20], which is averaged over categories, to evaluate the panoptic segmentation performance. PQ is the combination of recognition quality (RQ) and segmentation quality (SQ). PQTh averaged over thing categories and PQSt averaged over stuff categories are also reported to reflect the improvement on instance and semantic segmentation.

Implementation details. We choose Res50-FPN and Dcn101-FPN as our backbone for *val* and *test-dev* respec-

Method	Backbone	PQ	PQ Th	PQ St
<i>two-stage</i>				
Panoptic-FPN	Res101-FPN	40.9	48.3	29.7
AUNet	ResX152-FPN	46.5	55.9	32.5
UPSNet	Dcn101-FPN	46.6	53.2	36.7
Unifying	Dcn101-FPN	47.2	53.5	37.7
BANet	Dcn101-FPN	47.3	54.9	35.9
SOGNet	Dcn101-FPN	47.8	-	-
<i>one-stage</i>				
DeeperLab	Xception-71	34.3	37.5	29.6
SSAP	Res101-FPN	36.9	40.1	32.0
Panoptic-Deeplab	Xception-71	39.6	-	-
Axial-Deeplab	Axial-ResNet-L	43.6	48.9	35.6
Panoptic-FCN*	Dcn101-FPN	47.5	53.7	38.2
Ours*	Dcn101-FPN	48.1	55.6	36.7

Table 2: Results on COCO *test-dev* set.

tively. We set Fourier decomposition level N to 5 and reference spatial size S to 16 to well balance performance and efficiency. λ is set to 0.5. For fair comparison on MS COCO, we report performances obtained from 36 epochs training schedule following [24]. We use the SGD optimization algorithm with momentum of 0.9 and weight decay of $1e-4$. The batch-size is set to 16. For data augmentation, random crop and horizontal flip are used. As for inference, the score thresholds before and after NMS are set to 0.1 and 0.3. Stuff regions whose areas are below 4096 are removed [20]. For ADE20k, we merely adjust the training schedule. Following the setting of BGRNet [46], we train for 24 epochs with learning rate divided by 10 at the 18 and 22 epochs.

4.1. Comparison with State-of-the-Art Methods

We compare our method with state-of-the-art methods on COCO *val* and *test-dev* on the GPU device NVIDIA V100. Quantitative results on *val* are shown in Tab. 1

Method	Backbone	PQ	PQ Th	PQ St
<i>two-stage</i>				
Panoptic-FPN	Res50-FPN	29.3	32.5	22.9
Panoptic-FPN [†]	Res50-FPN	30.1	33.1	24.0
BGRNet	Res50-FPN	31.8	34.1	27.3
<i>one-stage</i>				
Ours*	Res50-FPN	32.6	35.0	27.9

Table 3: Results on ADE20k *val* set.

SCM	ICM	PQ	SQ	RQ	Inf (ms)
		39.3	77.6	48.3	84.3
✓		39.9	77.8	49.1	88.2
	✓	39.6	77.1	48.7	90.0
✓	✓	40.5	78.6	49.7	93.4

Table 4: Ablation Study on COCO *val* set.

and Fig. 6. We provide results without/with deformable convolutions, denoted as Ours and Ours* respectively. As one can tell in Tab. 1, Ours* based on Res50-FPN outperforms all the comparing single-stage methods in both accuracy and efficiency on COCO *val*. When compared to Panoptic-FCN, our method is 0.9% PQ higher with a higher running speed (+0.8FPS). With deformable convolutions, ours* exceeds two-single stage methods by 1.4% PQ and is still faster. In Tab. 2, we provide results on COCO *test-dev* subset. Ours* based on Dcn101-FPN outperforms all top-listed approaches and even exceeds the best two-stage SOGNet [52] by 0.3% PQ, showing the great potential of our method combined with a powerful backbone.

In Tab. 3, we compare our method with state-of-the-art methods on ADE20k *val*-set. Being the first single-stage method to provide results on ADE20k, our method outperforms previous two-stage methods by 0.8% higher PQ. It shows a stronger performance for both foreground and background regions, showing that our method is able to learn correlations effectively for different datasets.

4.2. Ablation Study

We perform ablation studies on COCO *val* with our model based on Res50-FPN. For efficiency, we train the model with a shorter training schedule (12 epochs) following [24] and do not employ Deformable Convolution. At first, we study the effectiveness of our correlation modules by adding them one-by-one to the baseline which directly attaches instance and semantic heads to the backbone features. Next, we study the importance of adapted correlation information by comparing them to existing Coord-Conv [28] and attention mechanism [40] on separate segmentation tasks. Finally, we give ablations on the choice of hyper-parameters and computational cost.

Semantic correlation module. To study the effect of semantic correlation module (SCM), we run experiments with SCM alone. As shown in the second row of Tab. 4, applying

methods	-	att	SCM
mIoU	47.6	50.1	50.7

Table 5: Ablation on SCM on COCO *val* set.

methods	-	coords	sinoduals	ICM
mIoU	29.5	32.9	32.5	33.5

Table 6: Ablation on ICM on COCO *val* set.

	Semantic			Instance(N=5)		
	N=3	N=5	N=7	S=8	S=16	S=32
mIoU	50.3	50.7	50.5	-	-	-
mAP	-	-	-	33.3	33.5	33.6

Table 7: Ablation on hyper-parameters on COCO *val* set.

SCM alone leads to a 0.6% gain in PQ. This mainly comes from the improved PQSt (+2.7%), showing that SCM is able to learn beneficial semantic correlation under the implicit supervision from semantic branch.

Instance correlation module. To study the effect of instance correlation module (ICM), we run experiments with ICM alone and with both ICM and SCM. As shown in the third row of Tab. 4, applying ICM alone leads to a 0.3% gain in terms of PQ. Such an increment can be attributed to the 0.5% higher PQTh. This demonstrates that ICM effectively models the correlation information suitable for instance segmentation. Since ICM needs to predict instance-level correlations from the backbone features and thus incorporating ICM alone into the one-stage framework may encourage the backbone features to become more instance-level discriminative and affect the semantic segmentation branch. More importantly, by jointly applying SCM and ICM, our performance is further increased by 0.6%. This reveals that our correlation modules are able to work together to provide task-specific scene-adaptive discriminative features to alleviate the intrinsic conflicts between two segmentation tasks, thus leading to better performance.

Task-driven and Scene-related correlation. To show the importance of task-driven and scene-related correlation information, we compare SCM and ICM with Coord-Conv [28] and attention mechanism [40] on instance and semantic segmentations separately. For semantic segmentation, the baseline is a backbone network with a segmentation head of 3 stacked 3×3 convs. And we incorporate self-attention [40] and SCM modules into the segmentation head in baseline denoted as “att” and “SCM”, respectively. As shown in Table 5, our method SCM outperforms “att” with a noticeable gain. For instance segmentation, the self-attention module may enhance the feature similarity for those locations belonging to the same semantic category and thus hinder instance-level discrimination. There-

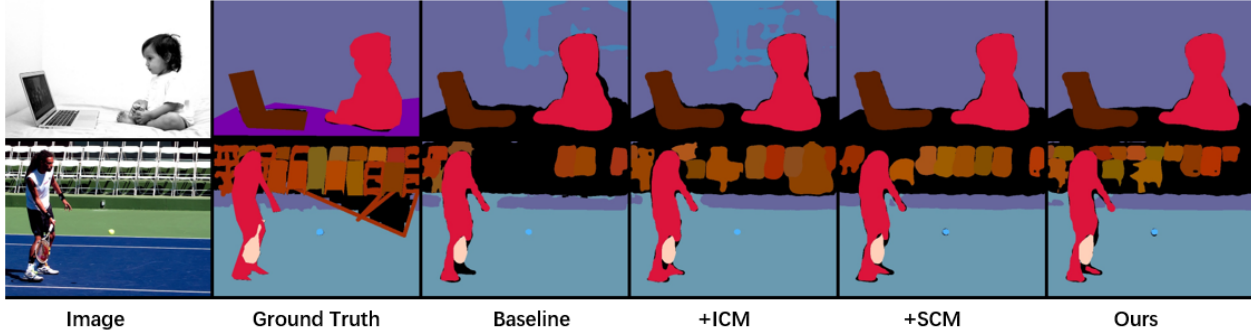


Figure 7: Qualitative results of different correlation modules on COCO.



Figure 8: Visualizations of the implicitly learned semantic (first row) and instance (second row) correlations. Each correlation map is obtained by calculating the correlation between each location and a fixed location (labeled as a green point) with a warmer color for a stronger correlation.

fore, we compare with coordinates [28] and sinoidal embeddings [2] based methods instead of self-attention methods. As shown in Tab. 6, our ICM obtains 33.5% mAP, 0.6% higher than using coordinates.

Hyper-parameters. There are two hyper-parameters in our proposed modules, namely the Fourier decomposition level N and spatial size of reference points S . We conduct ablation studies on these two hyper-parameters separately on semantic and instance segmentation. As shown in Tab. 7, the highest performance is achieved on semantic segmentation when N is set to 5. The DFT function could not approximate the correlations well when the N is too small. And a higher N may lead to overfitting. For instance segmentation, $S = 32$ is slightly better than $S = 16$. Taking efficiency into account, we set S to 16 in all experiments.

Ablation on computational cost. In this part, we perform an ablation study to demonstrate that the proposed method is more effective than using more extra computations or parameters. The baseline is based on Res50-FPN with a standard SOLO instance segmentation head and a segmentation head of 3 stacked 3×3 convs. To show the performance gain of our method is not obtained by merely adding more com-

Table 8: Ablation on extra parameters on COCO *val* set.

methods	PQ	SQ	RQ	Inf (ms)	Params (M)
Baseline	39.3	77.6	48.3	84.3	37.55
Deeper Head	39.9	78.2	48.9	93.3	38.88(+1.33)
Ours	40.5	78.6	49.7	93.4	38.15(+0.60)

putations or parameters, we make the segmentation head in baseline deeper to 7 convs, denoted as “Deeper Head”. As shown in Table 8, our method, with a similar runtime, outperforms “Deeper Head” with a noticeable gain w.r.t. **all metrics** and uses less parameters.

4.3. Visualizations

In this part, we provide some qualitative results to demonstrate the effectiveness of the proposed algorithm. We first demonstrate visual examples of the panoptic segmentation results obtained by our method in Fig. 7. In the first row, misclassified regions are corrected due to SCM. In the second row, ICM helps to identify missing instances, resulting in a higher RQ^{Th} . In addition, we give more visualizations of correlations learned implicitly by the proposed method. As one can tell in Fig. 8, our algorithm is able to capture task-specific and scene-related correlations for different segmentation tasks.

5. Conclusion

In this paper, we propose a novel approach for learning discriminative features via correlation functions for scene understanding tasks. It explicitly models the correlations as scene-relevant functions of locations and optimizes them through implicit supervisions. We further design two modules, namely semantic correlation module and instance correlation module to apply correlations in various segmentation tasks. These modules are integrated into an one-stage pipeline for efficient panoptic segmentation. The experimental results demonstrate that the proposed method is able to learn task-specific correlations flexibly, leading to state-of-the-art performances on COCO and ADE20k.

References

- [1] Dana H Ballard. Generalizing the hough transform to detect arbitrary shapes. *PR*, 13(2):111–122, 1981. 2
- [2] Nicolas Carion, Francisco Massa, Gabriel Synnaeve, Nicolas Usunier, Alexander Kirillov, and Sergey Zagoruyko. End-to-end object detection with transformers. In *ECCV*, 2020. 1, 8
- [3] Chia-Yuan Chang, Shuo-En Chang, Pei-Yung Hsiao, and Li-Chen Fu. Epsnet: Efficient panoptic segmentation network with cross-layer attention fusion. In *Proceedings of the Asian Conference on Computer Vision*, 2020. 2
- [4] L. Chen, G. Papandreou, I. Kokkinos, K. Murphy, and A. L. Yuille. Deeplab: Semantic image segmentation with deep convolutional nets, atrous convolution, and fully connected crfs. *IEEE TPAMI*, 40(4):834–848, 2018. 2
- [5] L. Chen, G. Papandreou, F. Schroff, and H. Adam. Rethinking atrous convolution for semantic image segmentation. *CoRR*, abs/1706.05587, 2017. 2
- [6] L. Chen, Y. Zhu, G. Papandreou, F. Schroff, and H. Adam. Encoder-decoder with atrous separable convolution for semantic image segmentation. In *ECCV*, pages 801–818, 2018. 2
- [7] Xinlei Chen, Ross Girshick, Kaiming He, and Piotr Dollár. Tensormask: A foundation for dense object segmentation. In *ICCV*, pages 2061–2069, 2019. 2
- [8] Xia Chen, Jianren Wang, and Martial Hebert. Panonet: Real-time panoptic segmentation through position-sensitive feature embedding. *CoRR*, abs/2008.00192, 2020. 2
- [9] Yifeng Chen, Guangchen Lin, Songyuan Li, Omar Bourahla, Yiming Wu, Fangfang Wang, Junyi Feng, Mingliang Xu, and Xi Li. Banet: Bidirectional aggregation network with occlusion handling for panoptic segmentation. In *CVPR*, pages 3793–3802, 2020. 2, 6
- [10] Bowen Cheng, Maxwell D. Collins, Yukun Zhu, Ting Liu, Thomas S. Huang, Hartwig Adam, and Liang-Chieh Chen. Panoptic-deeplab: A simple, strong, and fast baseline for bottom-up panoptic segmentation. In *CVPR*, June 2020. 1, 2, 6
- [11] J. Dai, H. Qi, Y. Xiong, Y. Li, G. Zhang, H. Hu, and Y. Wei. Deformable convolutional networks. In *ICCV*, pages 764–773, 2017. 2
- [12] Xuefeng Du, Chenhan Jiang, Hang Xu, Gengwei Zhang, and Zhenguo Li. How to save your annotation cost for panoptic segmentation? In *Proceedings of the AAAI Conference on Artificial Intelligence*, volume 35, pages 1282–1290, 2021. 1
- [13] Naiyu Gao, Yanhu Shan, Xin Zhao, and Kaiqi Huang. Learning category-and instance-aware pixel embedding for fast panoptic segmentation. *IEEE Transactions on Image Processing*, 30:6013–6023, 2021. 2, 6
- [14] K. He, G. Gkioxari, P. Dollár, and R. Girshick. Mask r-cnn. In *ICCV*, pages 2980–2988, 2017. 2
- [15] K. He, X. Zhang, S. Ren, and J. Sun. Deep residual learning for image recognition. In *CVPR*, pages 770–778, 2016. 3
- [16] Weixiang Hong, Qingpei Guo, Wei Zhang, Jingdong Chen, and Wei Chu. Lpsnet: A lightweight solution for fast panoptic segmentation. In *CVPR*, pages 16746–16754, 2021. 1, 6
- [17] Rui Hou, Jie Li, Arjun Bhargava, Allan Raventos, Vitor Guizilini, Chao Fang, Jerome Lynch, and Adrien Gaidon. Real-time panoptic segmentation from dense detections. In *CVPR*, pages 8523–8532, 2020. 2, 6
- [18] Zilong Huang, Xinggang Wang, Lichao Huang, Chang Huang, Yunchao Wei, and Wenyu Liu. Ccnet: Criss-cross attention for semantic segmentation. In *ICCV*, pages 603–612, 2019. 2
- [19] A. Kirillov, R. Girshick, K. He, and P. Dollár. Panoptic feature pyramid networks. In *CVPR*, pages 6392–6401, 2019. 1, 2, 6
- [20] A. Kirillov, K. He, R. Girshick, C. Rother, and P. Dollár. Panoptic segmentation. In *CVPR*, pages 9396–9405, 2019. 1, 2, 3, 6
- [21] Justin Lazarow, Kwonjoon Lee, Kunyu Shi, and Zhuowen Tu. Learning instance occlusion for panoptic segmentation. In *CVPR*, pages 10720–10729, 2020. 2
- [22] Qizhu Li, Xiaojuan Qi, and Philip HS Torr. Unifying training and inference for panoptic segmentation. In *CVPR*, pages 13320–13328, 2020. 2, 6
- [23] Y. Li, X. Chen, Z. Zhu, L. Xie, G. Huang, D. Du, and X. Wang. Attention-guided unified network for panoptic segmentation. In *CVPR*, pages 7019–7028, 2019. 2
- [24] Yanwei Li, Hengshuang Zhao, Xiaojuan Qi, Liwei Wang, Zeming Li, Jian Sun, and Jiaya Jia. Fully convolutional networks for panoptic segmentation. In *CVPR*, pages 214–223, 2021. 1, 6, 7
- [25] T. Lin, P. Dollár, R. Girshick, K. He, B. Hariharan, and S. Belongie. Feature pyramid networks for object detection. In *CVPR*, pages 936–944, 2017. 1, 3
- [26] T. Lin, M. Maire, S. Belongie, L. Bourdev, R. Girshick, J. Hays, P. Perona, D. Ramanan, C. Zitnick, and P. Dollár. Microsoft coco: Common objects in context. In *ECCV*, pages 740–755. Springer, 2014. 5
- [27] H. Liu, C. Peng, C. Yu, J. Wang, X. Liu, G. Yu, and W. Jiang. An end-to-end network for panoptic segmentation. In *CVPR*, pages 6165–6174, 2019. 2
- [28] Rosanne Liu, Joel Lehman, Piero Molino, Felipe Petroski Such, Eric Frank, Alex Sergeev, and Jason Yosinski. An intriguing failing of convolutional neural networks and the coordconv solution. In *Advances in Neural Information Processing Systems*, pages 9605–9616, 2018. 1, 2, 7, 8
- [29] Xiaolong Liu, Yuqing Hou, Anbang Yao, Yurong Chen, and Keqiang Li. Casnet: Common attribute support network for image instance and panoptic segmentation. In *2020 25th International Conference on Pattern Recognition (ICPR)*, pages 8469–8475. IEEE, 2021. 2
- [30] J. Long, E. Shelhamer, and T. Darrell. Fully convolutional networks for semantic segmentation. In *CVPR*, pages 3431–3440, 2015. 2
- [31] A. Newell, Z. Huang, and J. Deng. Associative embedding: End-to-end learning for joint detection and grouping. In *Advances in Neural Information Processing Systems*, pages 2277–2287, 2017. 2
- [32] Alan V Oppenheim. *Discrete-time signal processing*. Pearson Education India, 1999. 2

- [33] Lorenzo Porzi, Samuel Rota Buló, Aleksander Colovic, and Peter Kotschieder. Seamless scene segmentation. In *CVPR*, pages 8277–8286, 2019. [2](#)
- [34] Jiawei Ren, Cunjun Yu, Zhongang Cai, Mingyuan Zhang, Chongsong Chen, Haiyu Zhao, Shuai Yi, and Hongsheng Li. Refine: Prediction fusion network for panoptic segmentation. In *Proceedings of the AAAI Conference on Artificial Intelligence*, volume 35, pages 2477–2485, 2021. [1](#)
- [35] Konstantin Sofiiuk, Olga Barinova, and Anton Konushin. Adaptis: Adaptive instance selection network. In *ICCV*, October 2019. [1](#)
- [36] Zhi Tian, Chunhua Shen, and Hao Chen. Conditional convolutions for instance segmentation. In *ECCV*, 2020. [2](#)
- [37] Ashish Vaswani, Noam Shazeer, Niki Parmar, Jakob Uszkoreit, Llion Jones, Aidan N Gomez, Łukasz Kaiser, and Illia Polosukhin. Attention is all you need. In *Advances in Neural Information Processing Systems*, 2017. [2](#), [5](#)
- [38] Haochen Wang, Ruotian Luo, Michael Maire, and Greg Shakhnarovich. Pixel consensus voting for panoptic segmentation. In *CVPR*, pages 9464–9473, 2020. [2](#), [6](#)
- [39] Huiyu Wang, Yukun Zhu, Bradley Green, Hartwig Adam, Alan L. Yuille, and Liang-Chieh Chen. Axial-deeplab: Stand-alone axial-attention for panoptic segmentation. In *ECCV*, 2020. [2](#), [5](#)
- [40] Xiaolong Wang, Ross Girshick, Abhinav Gupta, and Kaiming He. Non-local neural networks. In *Proceedings of the IEEE conference on computer vision and pattern recognition*, pages 7794–7803, 2018. [7](#)
- [41] Xinlong Wang, Tao Kong, Chunhua Shen, Yuning Jiang, and Lei Li. SOLO: Segmenting objects by locations. In *ECCV*, 2020. [1](#), [2](#), [3](#), [4](#)
- [42] Xinlong Wang, Shu Liu, Xiaoyong Shen, Chunhua Shen, and Jiaya Jia. Associatively segmenting instances and semantics in point clouds. In *Proceedings of the IEEE/CVF Conference on Computer Vision and Pattern Recognition*, pages 4096–4105, 2019. [2](#)
- [43] Xinlong Wang, Rufeng Zhang, Tao Kong, Lei Li, and Chunhua Shen. Solov2: Dynamic, faster and stronger. In *Advances in Neural Information Processing Systems*, 2020. [2](#), [3](#), [6](#)
- [44] Zhenyi Wang and Olga Veksler. Location augmentation for CNN. *CoRR*, abs/1807.07044, 2018. [1](#), [5](#)
- [45] Boxi Wu, Shuai Zhao, Wenqing Chu, Zheng Yang, and Deng Cai. Improving semantic segmentation via dilated affinity. *arXiv preprint arXiv:1907.07011*, 2019. [2](#)
- [46] Yangxin Wu, Gengwei Zhang, Yiming Gao, Xiajun Deng, Ke Gong, Xiaodan Liang, and Liang Lin. Bidirectional graph reasoning network for panoptic segmentation. In *CVPR*, pages 9080–9089, 2020. [2](#), [6](#)
- [47] Enze Xie, Peize Sun, Xiaoge Song, Wenhai Wang, Xuebo Liu, Ding Liang, Chunhua Shen, and Ping Luo. Polarmask: Single shot instance segmentation with polar representation. In *CVPR*, 2020. [2](#)
- [48] Y. Xiong, R. Liao, H. Zhao, R. Hu, M. Bai, E. Yumer, and R. Urtasun. Upsnet: A unified panoptic segmentation network. In *CVPR*, pages 8810–8818, 2019. [2](#), [3](#), [6](#)
- [49] Wenqiang Xu, Haiyang Wang, Fubo Qi, and Cewu Lu. Explicit shape encoding for real-time instance segmentation. In *ICCV*, 2019. [2](#)
- [50] Brandon Yang, Gabriel Bender, Quoc V Le, and Jiquan Ngiam. Condconv: Conditionally parameterized convolutions for efficient inference. In *Advances in Neural Information Processing Systems*, pages 1307–1318, 2019. [2](#)
- [51] Tien-Ju Yang, Maxwell D Collins, Yukun Zhu, Jyh-Jing Hwang, Ting Liu, Xiao Zhang, Vivienne Sze, George Papandreou, and Liang-Chieh Chen. Deeperlab: Single-shot image parser. *arXiv preprint arXiv:1902.05093*, 2019. [6](#)
- [52] Yibo Yang, Hongyang Li, Xia Li, Qijie Zhao, Jianlong Wu, and Zhouchen Lin. Sognet: Scene overlap graph network for panoptic segmentation. In *Proceedings of the AAAI Conference on Artificial Intelligence*, volume 34, pages 12637–12644, 2020. [2](#), [6](#), [7](#)
- [53] Hui Ying, Zhaojin Huang, Shu Liu, Tianjia Shao, and Kun Zhou. Embedmask: Embedding coupling for one-stage instance segmentation. *CoRR*, abs/1912.01954, 2019. [2](#)
- [54] Gengwei Zhang, Yiming Gao, Hang Xu, Hao Zhang, Zhen-guo Li, and Xiaodan Liang. Ada-segment: Automated multi-loss adaptation for panoptic segmentation. In *Proceedings of the AAAI Conference on Artificial Intelligence*, volume 35, pages 3333–3341, 2021. [1](#)
- [55] H. Zhao, J. Shi, X. Qi, X. Wang, and J. Jia. Pyramid scene parsing network. In *CVPR*, pages 6230–6239, 2017. [2](#)
- [56] Shuai Zhao, Yang Wang, Zheng Yang, and Deng Cai. Region mutual information loss for semantic segmentation. In *Advances in Neural Information Processing Systems*, volume 32, pages 11117–11127, 2019. [2](#)
- [57] Shuai Zhao, Boxi Wu, Wenqing Chu, Yao Hu, and Deng Cai. Correlation maximized structural similarity loss for semantic segmentation. *arXiv preprint arXiv:1910.08711*, 2019. [2](#)
- [58] Bolei Zhou, Hang Zhao, Xavier Puig, Sanja Fidler, Adela Barriuso, and Antonio Torralba. Scene parsing through ADE20K dataset. In *CVPR*, 2017. [5](#)